Differential reflectance and second-harmonic generation of the Si/SiO_2 interface from first principles

V. I. Gavrilenko
Center for Materials Research, Norfolk State University, 700 Park Avenue, Norfolk, Virginia 23504, USA
(Received 10 October 2007; published 9 April 2008)

The equilibrium atomic geometries of a Si/SiO_2 interface are studied by using first principles pseudopotential method within the density functional theory. The optical linear [reflectance differential spectra (RDS)] and nonlinear [second-harmonic generation (SHG)] spectra of the Si/SiO_2 interface are calculated using *ab initio* ultrasoft and norm-conserving pseudopotentials. Local bridgelike oxygen atomic configurations provide well defined optical features in both linear (RDS) and nonlinear (SHG) optical spectra of the Si/SiO_2 interface. The results of the present work demonstrate that it is possible to unambiguously identify spectral features in both linear (RDS) and nonlinear (SHG) optical spectra of the Si/SiO_2 interface with local atomic oxygen-related configurations. The advantages of a simultaneous analysis of RDS and SHG spectra are demonstrated in order to obtain a detailed picture of the Si/SiO_2 interface at the atomic level.

DOI: 10.1103/PhysRevB.77.155311 PACS number(s): 78.66.−w, 42.65.Ky, 73.20.−r

I. INTRODUCTION

The increasing amount of high-quality works on a Si/SiO_2 system within the past few years is caused by the extensive development of nanostructured electronics, which requires a good understanding of the processes at the atomic monolayer scale. An understanding of the oxygen-related processes on the Si/SiO_2 interface is very important for both fundamental and applied physics as well as for high-technology electronics. For a contactless optical characterization of the interface at the nanometer scale, the following nontraditional methods of optical spectroscopy are used: linear optical reflectance differential spectroscopy (RDS) (see Refs. 1–4 and references therein) and/or nonlinear optical spectroscopy methods, such as second-harmonic generation (SHG) (for details, see the review in Ref. 5). For the next generation of optical metrology, it is very important to have a detailed understanding of the optical spectra based on microscopic modeling and simulations. The first principles theories of RDS (Refs. 3 and 4) and SHG (Refs. 5 and 6) of silicon-based interfaces allowed substantial progress in our understanding of the physics and chemistry of the systems. However, such works are still rare (in particular, those related to the SHG) because they normally require extensive large-scale computations.[5,6] The atomic structure of the intermediate Si and SiO_2 layers is still extensively debated in the literature.[7,8] Monte Carlo simulations[7] and first principles modeling, based on density functional theory (DFT) and total energy minimization method,[8] confirmed the ordered Si-O-Si bridge structure as a basic unit of the intermediate SiO_2 layer. On the other hand, the Rutherford ion scattering data, which were measured on the Si/SiO_2 interface and interpreted using the *ab initio* DFT study with a modified interatomic potential,[9] suggested a substantial contribution of a disordered interface structure. It should be noted that optical spectra are very sensitive to structural disorder, which smears out well-pronounced atomic order-related features.

The RDS data measured on a Si surface exposed to oxygen adsorption are strongly modified in the region between 3.4 and 4.0 eV. Well-pronounced RDS peaks are interpreted as the result of breaking the dimer bonds on Si(001) followed by the creation of a bridge oxygen structure.[1,2] The SHG spectra, which were measured on the systems containing single[10] or multiple $Si(001)/SiO_2$ interfaces (multiple Si/SiO_2 quantum wells[11]), included SHG features in the spectral region near 2.7 eV (Ref. 11) and 3.8 eV (Refs. 10 and 11), which could not be interpreted in terms of the perturbations of the Si bulklike direct electron gaps.

A realistic modeling of optical functions of solid surfaces and interfaces still remains challenging for the first principles theories.[3–5] A description of excited states, which could be in good agreement with experiment, normally requires the inclusion of local field, many-body (excitons) effects, and, probably, other nonlocal contributions (particularly for SHG).[12,13] This makes theory much more complicated than the frequently used independent particle approach [or random phase approximation (RPA)]. The nonlinear SHG response from the surfaces and interfaces is more challenging for the *ab initio* theory even within the RPA method because of the more complicated unit cell. Consequently, first principles studies of the SHG from solid surfaces are still rare (see Refs. 5, 6, and 12, and references therein).

This work presents the results of an extensive first principles large-scale computational analysis of both linear (RDS) and nonlinear (SHG) optical spectra of the Si/SiO_2 interface. The results demonstrate the possibility of unambiguously identifying well-pronounced spectral features in both RDS and SHG optical spectra of the Si/SiO_2 interface with local atomic oxygen-related configurations.

II. METHOD

The equilibrium atomic structures of the $Si(001)/SiO_2$ interface are obtained from the total energy minimization method within DFT by using *ab initio* norm-conserving pseudopotentials (PPs) presented in the CASTEP package.[14] The Si(001) surface is modeled by a 12 monolayer (ML) slab, of which the top six layers were allowed to relax. The eigenvalue problem was solved using the open-source first principles pseudopotential based packages[15,16] [norm-

conserving PP (NC-PP)] and VASP (Ref. 17) [ultrasoft PP (USP)]. Convergence of the results has been carefully checked by choosing energy cutoff values up to 70 Ry. The cutoff energy of 40 Ry was chosen for NC-PP to ensure reliable convergence of predicted optical data. Almost the same accuracy is achieved with a cutoff energy of 30 Ry for USP. This is in agreement with previous findings.[3,4] The same cutoff energy is used for both the generation of pseudopotentials and computations. The choice of pseudopotentials (USP or NC-PP) does not significantly affect the results. An exchange and correlation interaction is modeled according to Ref. 18. A quasiparticle (QP) scissorlike correction of 0.5 eV is required to obtain predicted direct optical gap energies of 3.4 eV (E_1) for a 12 ML Si slab, which agrees with a previous finding that used a similar theoretical framework for the Si(001) surface.[3,4]

Calculated self-consistent eigenenergies and eigenfunctions are used as inputs for optical calculations. Within its penetration depth beneath the surface, the incident light field at frequency ω [$E(\omega)$] induces different order optical susceptibilities $\chi^{(n)}$ of linear and second order polarizations of the following forms:[5]

$$P_i(\omega) = \chi_{ij}^{(1)} E_j(\omega), \tag{1}$$

$$P_i(2\omega) = \chi_{ijk}^{(2)} E_j(\omega) E_k(\omega) + \chi_{ijkl}^{(3)} E_j(\omega) \nabla_k E_l(\omega) + \chi_{ijkl}^{(3)} E_j(\omega) E_k(\omega) E_l^{dc}. \tag{2}$$

Equation (1) presents a linear dipole polarization describing different linear response functions. Experimentally, the surface sensitive linear optical RDS signal is measured as a normalized difference between two reflectance coefficients when the incoming light is polarized along two mutually perpendicular in-surface vectors (e.g., for the (001) surface, the two vectors are [110] and $[1\bar{1}0]$).[1] The theory of RDS from solid surfaces was given earlier.[19] A linear optical RDS response is determined through the diagonal components of the optical polarizability function α as follows:[19]

$$\frac{\Delta R_\alpha(\omega)}{R_0(\omega)} = \frac{4\omega}{c} \mathrm{Im}\left[\frac{4\pi \alpha_{\alpha\alpha}^{hs}}{\varepsilon_b(\omega) - 1} \right]. \tag{3}$$

The average diagonal elements of $\alpha_{\alpha\alpha}$ are determined through the dielectric susceptibility function ε of bulk (index b) and through the $\chi_{\alpha\alpha}^{(1)}$ function in Eq. (1) of the upper half-slab (index hs).[19] Earlier,[5] we described how to account for the contributions of only one light exposing half of the slab.

Nonlinear optical response, originating from anharmonic bond polarizabilities, governs SHG and is determined through several contributions given by Eq. (2). The first term in Eq. (2) describes the second order optical excitation process and vanishes in centrosymmetric systems (such as bulk Si). Two other contributions are nonlocal and normally very weak. The second term, which is proportional to the field gradient (∇E), is the electric quadrupole component (in magnetic materials, it also contains a magnetic dipole component). The external electric field (if present) E^{dc} breaks central symmetry, thus inducing a SHG (and even higher order) response. In bulk Si, only the two last terms in Eq. (2) contribute to the SHG, resulting in a very weak signal.[5]

In the surface area, the symmetry is broken due to the crystal truncation, thus allowing the contribution of the first term in Eq. (2). The electric field induced second harmonic (EFISH) [third term in Eq. (2)] originating, e.g., from charge redistribution in the surface area, surface defects and impurities, external electric field, etc., is believed to provide a remarkable contribution to the SHG signal in some cases.[10,20]

Another nonlocal contribution to the SHG originating from exciton and local-field effects was recently studied.[12] At present, this much more complicated theory of SHG could be applied to relatively simple bulk systems. The inclusion of exciton and local-field effects in the SHG theory of bulk GaAs improves the agreement with experiment; however, these contributions are still insufficient to account for the differences observed.[12] Because of the extreme complexity of the surface SHG, the nonlocal contributions to optical functions are currently out of the scope of the present study.

Linear and nonlinear optical susceptibility functions are calculated in this work in the longitudinal gauge as formulated by Sipe and co-workers in Refs. 21 and 22. A detailed study of the different approaches in the evaluation of SHG based on longitudinal or velocity gauges shows their equivalence.[12] By oblique incidence, the SHG efficiency is determined by several tensor components of $\chi_{ijk}^{(2)}$. For the (001) surface, the SHG efficiency for p-polarized incoming and outgoing light, R_{pp}, is determined by five nonvanishing $\chi^{(2)}$ tensor components: $\chi_{zzz}^{(2)}$, $\chi_{zxx}^{(2)}$, $\chi_{zyy}^{(2)}$, $\chi_{xxz}^{(2)}$, and $\chi_{yyz}^{(2)}$. The explicit expression for R_{pp} for the (001) surface in terms of all nonvanishing $\chi_{ijk}^{(2)}$ tensor components is given elsewhere.[5,23,24]

III. RESULTS AND DISCUSSION

In this work, the (2×2) unit cell has been used to model a clean Si(001) surface. It has been demonstrated before that this model realistically reproduces most of the significant features of the electronic structure and RDS spectra of the bare Si(001) surface.[4,5,25] The initial oxidation stage of Si(001) is characterized mainly by two local atomic configurations including oxygen atom: oxygen dimer bridge and oxidized back-bond configurations (see Refs. 1–4, 25, and 26, and references therein). One of the main goals of the present work is to demonstrate that it is possible to unambiguously identify certain spectral features in both linear (RDS) and nonlinear (SHG) optical spectra of the Si/SiO_2 interface by using the dimer bridge configuration.

A. Reflectance difference spectra

The RDS spectra are calculated in this work according to Eq. (3). It has been proven earlier (see, e.g., Refs. 2–4 and 26, and references therein) that early-stage oxygen adsorption on the Si(001) surface is characterized by two almost energetically equivalent atomic configurations: dimer bond and back-bond bridge oxygen geometries. Our findings confirm this result. In order to avoid contributions of dangling bonds in optics, the hydrogenated Si(001) surface is studied

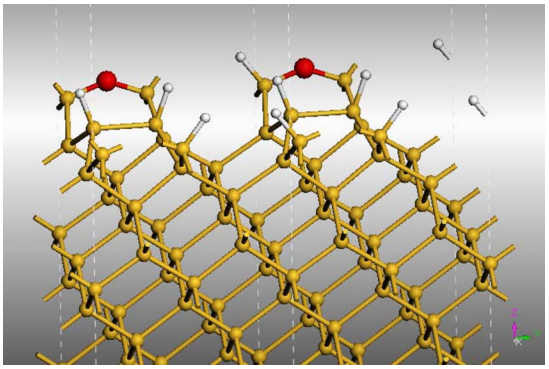

FIG. 1. (Color online) Atomic structure of Si(001) (2×2) surface with one local dimer oxygen configuration per unit cell. Red (dark grey) and white colored balls correspond to oxygen and hydrogen atoms, respectively.

in this work. The fully relaxed atomic structure of the hydrogenated Si(001) (2×2) surface with one local oxygen dimer bridge configuration per cell is shown in Fig. 1. The calculated value of the dimer length of 3.13 Å on a hydrogenated surface is slightly larger than the value of 3.06 Å on a Si(001) (2×2) surface without hydrogen obtained in Ref. 4. The calculated RDS spectrum of the hydrogenated Si(001) (2×2) surface exposed to oxygen is presented in Fig. 2. In order to better understand the effect of oxygen in optics, the RDS spectra calculated for surfaces with one and two bridge oxygen atoms per cell are shown for comparison. Due to the adsorption of hydrogen, all dangling bond-related electron states are pushed out of the gap area, thus removing the strong contribution to RDS in the long wavelength region. There is a weak RDS signal predicted in the region between 1.0 and 2.0 eV and a stronger response between 3 and 4 eV. The optical structure in the region between 3 and 4 eV was attributed to the contributions of back bonds.[25] The increase in the oxygen atom concentration dramatically enhances the signal in the region between 1.0 and 2.0 eV, which directly confirms the oxygen-related nature of this signal (see Fig. 2). This result agrees with the conclusion of Ref. 4, where the

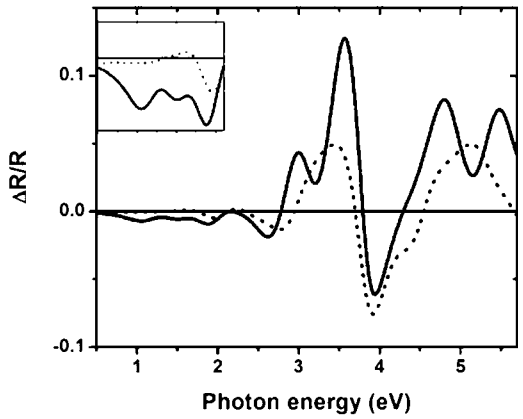

FIG. 2. Reflectance difference spectra of the hydrogenated Si(001) (2×2) surface with one (dashed) and two (solid) dimer oxygen atoms per unit cell. In the inset, the vertical scale of the low-energy region is expanded.

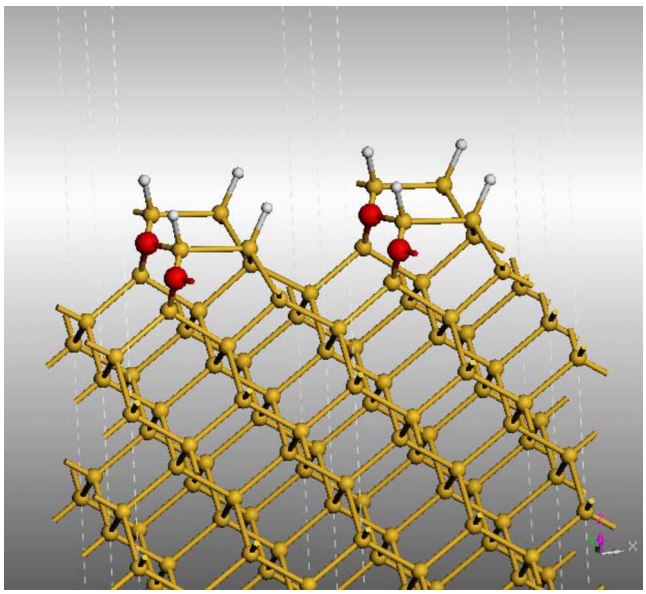

FIG. 3. (Color online) Atomic structure of Si(001) (2×1) surface with an oxygen atom located on a broken back bond. Red (dark grey) and white colored balls correspond to oxygen and hydrogen atoms, respectively.

calculated RDS signal at 1.5 eV was explained as oxygen-related optical excitations. The RDS response near 1.0 eV on hydrogen-free Si(001) is dominated by dangling bonds,[3,4,25] which masks possible oxygen-related contributions.

The equilibrium geometry of a bridge oxygen located in the broken back bonds of a monohydrate Si(001) surface is shown in Fig. 3. The length of the oxidized back bond on a hydrogenated surface (2.93 Å) is longer than that on a bare surface (2.61 Å). The latter agrees well with those reported earlier in the literature: 2.53 Å (Ref. 4) and 2.60 Å (Ref. 26). The calculated RDS spectrum of a back-bond bridge oxygen geometry is shown in Fig. 4 in comparison with the RDS spectrum predicted for a monohydrate Si(001) surface. It should be noted that the predicted RDS signal for the broken back-bond configuration has the opposite sign in the spectral region between 1 and 3 eV if compared to the bridge oxygen

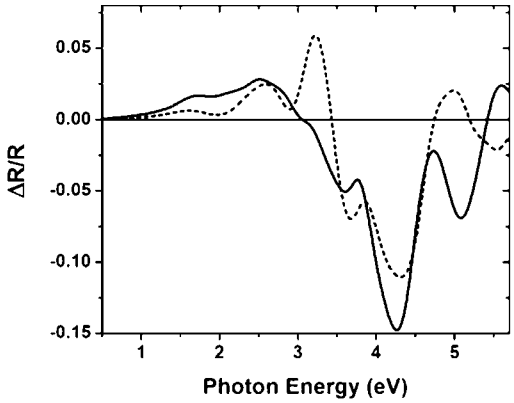

FIG. 4. Reflectance difference spectra of the hydrogenated Si(001) (2×1) surface with an oxygen atom located on a broken back bond (solid) is shown in comparison with a pure monohydrate (without oxygen) surface (dashed).

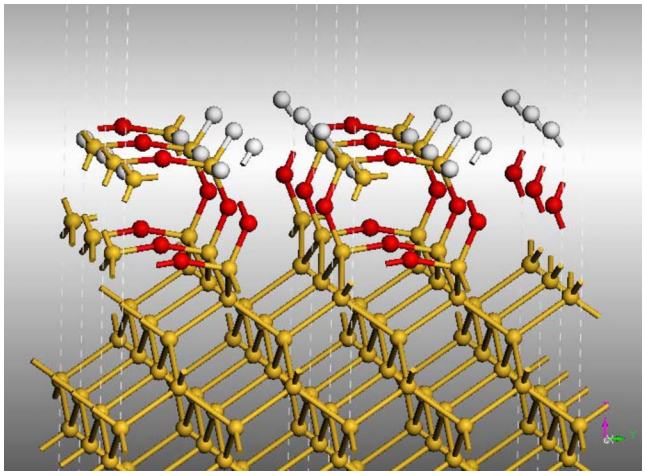

FIG. 5. (Color online) Fully relaxed atomic configuration of $Si(001)/SiO_2$ interface. Dashed lines indicate unit cells. Red (dark grey) and white colored balls correspond to oxygen and hydrogen atoms, respectively.

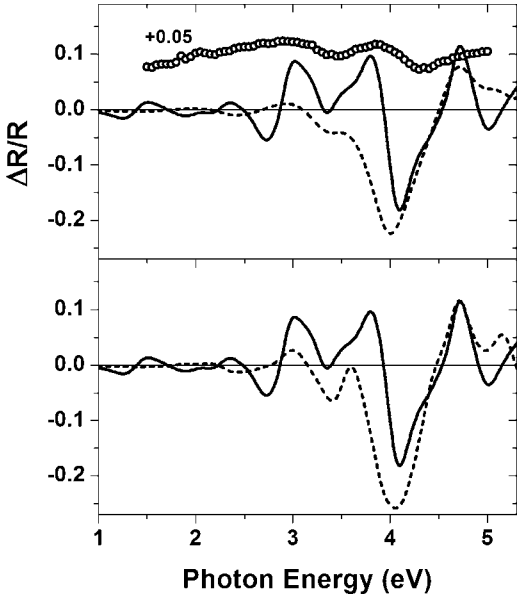

FIG. 6. Reflectance difference spectra of the $Si(001)/SiO_2$ interface corresponding to the fully relaxed interface atomic geometry given in Fig. 5 (solid lines) are shown in comparison to the RDS spectra calculated after the removal of the bridge oxygen (dashed lines). In the upper (lower) panel, the fully relaxed (unrelaxed) atomic structure of the $Si(001)/SiO_2$ interface without bridge oxygen is used for optical calculations. The experimental data of Ref. 1 are shifted upward by 0.05 for convenience.

geometry (see Fig. 2). For the broken back-bond configuration, one can see the enhancement of the RDS response in the region between 1.0 and 2.0 eV as similar to that obtained for the dimer bridge oxygen configuration. This response, however, does not completely disappear on a pure monohydrate Si(001) surface (see Fig. 4), indicating some contributions of distorted host atom back bonds in this spectral region. For a comparison of the linear (RDS) and nonlinear (SHG) optical spectra, it is interesting to note that the increase in the concentration of oxygen atoms located both on back bonds and dimer bridges strongly affects the RDS signal at around 3.6–3.8 eV (see Figs. 2 and 4). Bulk Si does not have any optical singularity in this region, which could, therefore, be identified as a surface oxygen-related contribution to the optical response.

The calculated tridymite atomic configuration of SiO_2 is used as a basic structural model for the initial oxide layer in the Si(001) surface. The fully relaxed atomic geometry of the $Si(001)/SiO_2$ interface is shown in Fig. 5. The atomic structure presented in Fig. 5 corresponds to the earlier reported atomic configuration for the tridymite.[8,27]

Previous studies of the Si/SiO_2 interface and the initial oxidation stage indicated that local atomic configurations with and without bridge dimer oxygen may coexist.[3,4,25,26] In order to understand the contribution of selected orbitals of a specific atom in the unit cell to the optical spectra, one can remove the atom of interest and perform electronic structure and optical function calculations. A comparison of energy structure and optics predicted with and without geometry optimization can help separate the effects of structural reconstruction (and local stress) and chemical hybridization. Local strains induce remarkable optical anisotropy on Si(001), as demonstrated in Ref. 3. In order to separately study the effects of local strains and chemical bond hybridization, in this work optical spectra are calculated for both relaxed and unrelaxed structures after the removal of a specific atom in the unit cell. The contributions of different atoms in the unit cell to optical response functions are also analyzed. It appears that the signature of the dimer bridge oxygen local configuration could be identified from the analysis of both linear and nonlinear optical spectra. This structure is created at the initial oxidation step after breaking the Si-Si dimer bond on the Si(001) surface by approaching the oxygen atom and creating the Si-O-Si dimer structure,[3,4] as presented in the tridymite oxide structure.[8,27]

First, the RDS spectra are considered. The goal is to relate the predicted local atomic configurations of the Si/SiO_2 interface to specific features observed in linear and nonlinear optical spectra. We discuss the calculated and measured linear optical RDS data presented in Fig. 6. The experimental RDS spectra shown in the upper panel of Fig. 6 are measured on Si(001) after room temperature adsorption of 160 Langmuir ($1L=1\times10^{-6}$ torr. sec) molecular oxygen.[1] The spectral positions between predicted (with a QP correction of 0.5 eV) and measured RDS optical peaks are in good agreement. Structural disorder apparently smears out the optical spectra, which may explain the substantial disagreement in a region around 4.0 eV. In Ref. 2, the evolution of RDS spectra with layer-by-layer oxide growth was studied. With an increase in the oxide thickness, the RDS peaks approach the spectral positions of the main peaks in bulk Si, thus indicating that the main contribution to optical anisotropy comes from the distorted back bonds. This is in agreement with the conclusion that was made earlier by a first principles study of the Si(001)+O system.[3]

The removal of the bridge oxygen substantially suppresses the RDS response. Calculations on a structurally relaxed system (see upper panel of Fig. 6) show that mechanical stress can cause some spectral shifts and a minor

redistribution of the oscillator strengths. However, a remarkable decrease in RDS response in the spectral region between 3 and 4 eV presented in both relaxed and unrelaxed (model) systems (lower panel of Fig. 6) could be understood as a result of oxygen-related rehybridization of back bonds, which demonstrates that the bridge dimer oxygen configuration could, indeed, provide a substantial contribution to the measured RDS signal, as assumed in Ref. 1. Another important result of the calculation is related to the predicted weak optical RDS structures located at around 2.3 and 1.4 eV. These peaks almost completely disappeared after the removal of the bridge oxygen (see Fig. 6). Borensztein *et al.*[1] reported that the weak RDS feature near 2.2 eV measured on Si/SiO_2 (shown in Fig. 2) is repeatedly reproduced in their experiments. However, because of the very low signal intensity, it was only assumed in Ref. 1 that this peak appears as a result of the oxidation. Based on the comparison with present results, the weak RDS structures measured near 2.2 eV, as well as those predicted at 2.3 and 1.4 eV, are related to the bridge oxygen as well. As discussed in detail above, the RDS peak at 1.5 eV that is related to the bridge dimer oxygen configuration was predicted in Ref. 4 and is confirmed in this work.

B. Second-harmonic generation

It was demonstrated earlier[3,20,21,28,29] that SHG is a unique method to study centrosymmetric solid surfaces: the SHG response is forbidden in bulk, and the SHG signal is generated within only a few surface monolayers. Because of this, one can expect a stronger contribution of the oxygen-related process in the $Si(001)/SiO_2$ interface to the SHG spectra than in linear optics. The calculated SHG efficiency spectra are now compared with available experimental data. Note that both the SHG and RDS data are calculated using the same eigenvalues and eigenvectors corresponding to the thridymite interface structure shown in Fig. 5. The SHG spectra measured on the Si(001) surface with native oxide[20] and on $Si(001)/SiO_2$ with potassium- and NaCl-covered oxides (in order to study the electric field effect in the space charge region[8]) indicate a strong dependence of the signal on the surface electric field and the appearance of a different optical structure in the region between 3.6 and 3.8 eV. EFISH offers incredible possibilities for the next generation of the optical metrology of the interfaces because of the high sensitivity of the SHG signal to the surface electric field.[9,27] From a theoretical perspective, however, the microscopic theory of EFISH is nonlocal, and it is still challenging for first principles theory.[3,25] Therefore, EFISH is beyond the scope of the present study. Here, we are focused on the effect of the chemical nature of electronic bond contributions on the $Si(001)/SiO_2$ interface to the SHG.

In Fig. 7, we present the calculated SHG spectra of the $Si(001)/SiO_2$ interface shown in Fig. 5. As expected, the nonzero SHG response is predicted only in the spectral region corresponding to optical two-photon excitations of the disturbed Si electron orbitals located near the surface. Due to the high value of the Si-O bond energy, corresponding contributions are located in the far ultraviolet region. The SHG

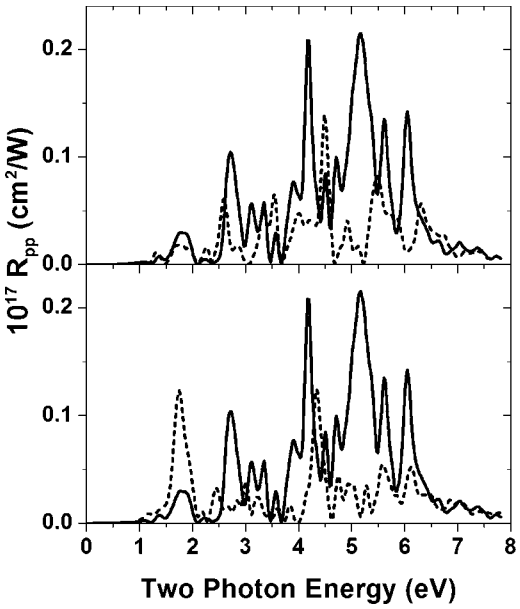

FIG. 7. Calculated SHG efficiency spectra of the $Si(001)/SiO_2$ interface corresponding to the fully relaxed interface atomic geometry given in Fig. 5 (solid line) are shown in comparison to the SHG spectra calculated after the removal of the bridge oxygen (dashed line). In the upper (lower) panel, the fully relaxed (unrelaxed) atomic structure of the $Si(001)/SiO_2$ interface without bridge oxygen is used for optical calculations (dashed lines).

response from the Si/SiO_2 interface, located mostly in visible and near-UV regions, is attributed to the distorted host atomic bonds.[3,24,29,30] From the data presented in Fig. 7, one can immediately extract features related to oxygen. The removal of the bridge oxygen results in dramatic reductions in the SHG features near 2.7, 3.3, 3.8–4.0, and 5.1 eV. A comparison between relaxed and unrelaxed structure calculations of the SHG efficiency (upper and lower panels in Fig. 7, respectively) shows that the effect of mechanical stress is much more pronounced in SHG than in RDS spectra (see Figs. 6 and 7). There are spectral shifts (see, e.g., E_2 optical structure near 4.0 eV) and a substantial redistribution of oscillator strengths. The optical SHG peak near 1.8 eV, which is related to the dimer bonds on the surface, is decreased after structural relaxation (see Fig. 7).

The SHG features near 3.3 and 5.1 eV are close to the bulk electron transitions E_1 and E_1'. Note that our theory with the QP correction predicts critical point energies in a Si slab at the following energies: $E_1=3.4$ eV, $E_2=4.15$ eV, and $E_1'=5.0$ eV. The peaks near 3.3 and 5.1 eV are apparently related to the bulklike electron excitations. According to the present work, the SHG response near 5.1 eV exhibits the strongest sensitivity to oxygen. However, this spectral region is still unavailable for experimental study. The SHG peak near 1.8 eV has a surface nature related to the Si dimer bond. This peak is strongly affected by oxygen and local stress (see Fig. 7). Although for this region the contribution of oxygen is clearly shown in the RDS spectra, in this spectral range the effect of stress relaxation is much less important in RDS than in SHG. The SHG peaks located near 2.7 and 3.8 eV are not predicted on the Si surfaces without oxygen. According to

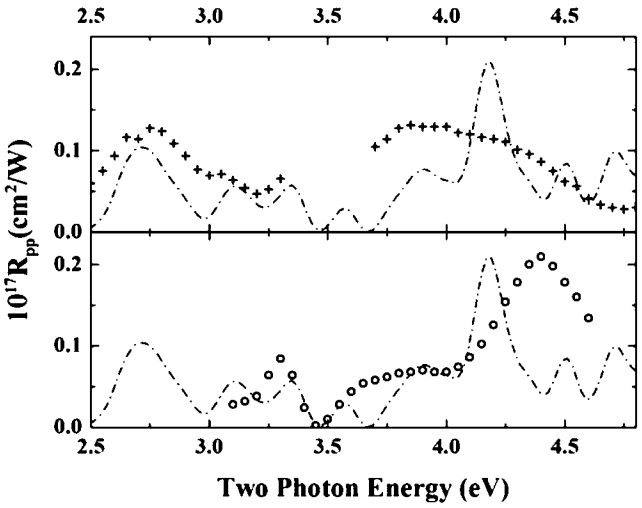

FIG. 8. Calculated SHG efficiency spectra of the $Si(001)/SiO_2$ interface in comparison with experimental data measured on an oxidized Si(001) surface (Ref. 10) (lower panel) and on $Si(001)/SiO_2$ multiple quantum well structures (Ref. 11) (upper panel).

our analysis of the projected density of states (PDOS) spectra, these peaks are directly related to the Si back bonds of the dimer atoms hybridized to the bridge oxygen $2p$ electrons. The peak near 4.0 eV is close to the E_2 transition and is strongly affected by the feature near 3.8 eV. A comparison between the SHG efficiency predicted for relaxed and unrelaxed tridymite structures after the removal of a bridge oxygen (upper and lower panels in Fig. 7, respectively) demonstrates that the effects of local stresses and bond rehybridization are equally important in SHG, which is in contrast to the RDS response.

The predicted SHG efficiency spectrum of an oxidized Si(001) surface is compared next to available experimental data.[9,10,20] In Fig. 8, we present a comparative analysis of the SHG spectra measured on two different systems: a Si(001) surface oxidized[10] or with natural oxide[28] and a Si/SiO_2 multiple quantum well (MQW) structure.[11] In order to compare the shape of the predicted and measured SHG spectra, the amplitudes of experimental data were scaled to meet the theoretical values at 4.2 eV (lower panel) and at 2.7 eV (upper panel). The experimental SHG spectrum shown in the upper panel in Fig. 8 was measured in Ref. 10 on a Si(001) sample with a 10 nm oxide layer grown by thermal oxidation at 1000 °C. The dominant SHG peak at 4.3 eV was attributed to the E_2 bulk transitions.[10] Note that the theoretical bulk value of E_2=4.15 eV underestimates the experimental one by about 0.1 eV. The results shown in Fig. 8 indicate the appearance of a SHG response in the region of 3.6–4.0 eV and a strong enhancement of the E_2 peak. A comparison with SHG data presented in Fig. 7 indicates that this is a combined effect of the oxygen-related rehybridization of Si back bonds and structural reconfiguration. A strong enhancement of both measured and predicted SHG efficiencies due to the effect of boron doping of the Si(001) surface (which was obtained on a relaxed system) was reported earlier.[20] In both cases, by neglecting the electric field effect, the physical nature of the predicted strong enhancement of the SHG efficiency is the impurity-related rehybridization and structural reconfiguration of the Si back bonds.

The predicted SHG response of 3.6–4.0 eV is also accompanied by a dramatic increase of the calculated SHG efficiency at 2.7 eV due to the dimer bridge oxygen (see Figs. 7 and 8). This part of the predicted SHG spectra agrees well with another type of experimental results. In Ref. 11, strong SHG signals were measured in the region near 2.7 eV on $Si(001)/SiO_2$ MQWs. In a MQW system, the quantum size effect is an additional factor affecting the SHG. However, in the presence of multiple $Si(001)/SiO_2$ boundaries, the effect of the interface oxygen should be enhanced. In the absence of microscopic theory, the 2.7 eV SHG signal measured in the $Si(001)/SiO_2$ MQW was interpreted in Ref. 11 as a result of electron transitions from the bounded quantum electron states in a quantum well. In addition to the quantum size effect, the chemical nature of the last SHG feature was also suggested in Ref. 11 as an alternative interpretation of their data. The results of the present work suggest that the origin of the measured[11] and predicted SHG responses near 2.7 eV is a dominant contribution of the rehybridized and reconstructed Si back bonds due to the creation of the dimer bridge oxygen structure on the $Si(001)/SiO_2$ interface. An additional argument regarding the current interpretation of the 2.7 eV signal is that this response should be accompanied by the SHG features near 3.8 eV, as discussed above (see Fig. 7). The experimental data of Ref. 11 confirm this rule: In addition to the 2.7 eV SHG peak, authors reported a strong SHG response at around 3.8–4.0 eV, which is discussed above.

An analysis of the atom- and orbital-resolved PDOS calculated in this work clearly indicates a strong effect of the bridge oxygen, which results in an additional contribution (hybridization) of oxygen p orbitals and silicon back-bond orbitals. The $2p$ orbitals of the bridge oxygen contribute to the top of the valence band. Modifications of the c band are less pronounced. The rehybridization of the host valence electron orbitals caused by both $2p$ orbitals of oxygen and structural distortions seems to be responsible for the measured and predicted optical anisotropies of this system. The dominating effect in the optical anisotropy of Si(001) due to the distorted back bonds and additional hybridization to oxygen has been shown in Ref. 3.

Finally, it should be noted that the effects of electric fields and, eventually, many-body (excitonic) and local-field effects should be incorporated into the nonlocal theory of the SHG in order to achieve a more detailed quantitative description of the signal shape, which should be considered as a future activity road map in the field. For future experimental and theoretical studies, it is important to note that a simultaneous analysis of RDS and SHG spectra has clear advantages for obtaining a detailed picture at the atomic level, as demonstrated in the present work.

IV. CONCLUSIONS

The equilibrium atomic structure and optical linear (RDS) and nonlinear (SHG) spectra of a Si/SiO_2 interface are stud-

ied using first principles density functional theory. A strong effect of oxygen adsorption on RDS and SHG spectra is predicted in visible and near-ultraviolet spectral regions. A comparative analysis of calculated and measured RDS and SHG optical spectra of the $Si(001)/SiO_2$ interface allows the identification of several spectral features as those related to the dimer bridge oxygen local atomic configuration of the $Si(001)/SiO_2$ interface. It is demonstrated that structural reconstructions of the host atomic bonds in the surface layers provide a much stronger effect in nonlinear (SHG) than in linear (RDS) optical spectra.

ACKNOWLEDGMENTS

This work is supported by NASA CREAM Grant No. NCC3-1035, NSF CREST supplement Grant No. HRD-0520208, NSF PREM DRM-0611430, and NSF NCN EEC-0228390.

[1] Y. Borensztein, O. Pluchery, and N. Witkowski, Phys. Rev. Lett. **95**, 117402 (2005).
[2] T. Yasuda, S. Yamasaki, M. Nishizawa, N. Miyata, A. Shklyaev, M. Ichikawa, T. Matsudo, and T. Ohta, Phys. Rev. Lett. **87**, 037403 (2001).
[3] F. Fuchs, W. G. Schmidt, and F. Bechstedt, Phys. Rev. B **72**, 075353 (2005).
[4] A. Incze, R. Del Sole, and G. Onida, Phys. Rev. B **71**, 035350 (2005).
[5] M. C. Downer, B. S. Mendoza, and V. I. Gavrilenko, Surf. Interface Anal. **31**, 966 (2001).
[6] H. Sano and G. Mizutani, e-J. Surf. Sci. Nanotechnol. **1**, 57 (2003).
[7] Y. Tu and J. Tersoff, Phys. Rev. Lett. **89**, 086102 (2002).
[8] R. Buczko, S. J. Pennycook, and S. T. Pantelides, Phys. Rev. Lett. **84**, 943 (2000).
[9] A. Bongiorno, A. Pasquarello, M. S. Hybertsen, and L. C. Feldman, Phys. Rev. Lett. **90**, 186101 (2003).
[10] A. Rumpel, B. Manschwetus, G. Lilienkamp, H. Schmidt, and W. Daum, Phys. Rev. B **74**, 081303(R) (2006).
[11] V. G. Avramenko, T. V. Dolgova, A. A. Nikulin, A. A. Fedyanin, O. A. Aktsipetrov, A. F. Pudonin, A. G. Sutyrin, D. Yu. Prokhorov, and A. A. Lomov, Phys. Rev. B **73**, 155321 (2006).
[12] R. Leitsmann, W. G. Schmidt, P. H. Hahn, and F. Bechstedt, Phys. Rev. B **71**, 195209 (2005).
[13] V. I. Gavrilenko and F. Bechstedt, Phys. Rev. B **55**, 4343 (1997).
[14] Accelrys, *Material Studio Release Notes, Release 4.2*, (Accelrys Software Inc., San Diego, CA, 2007).
[15] M. Fuchs and M. Scheffler, Comput. Phys. Commun. **119**, 67 (1999).
[16] N. Troullier and J. L. Martins, Phys. Rev. B **43**, 1993 (1991).
[17] G. Kresse and J. Furthmüller, Comput. Mater. Sci. **6**, 15 (1996).
[18] J. P. Perdew, K. Burke, and M. Ernzerhof, Phys. Rev. Lett. **77**, 3865 (1996).
[19] F. Manghi, R. Del Sole, A. Selloni, and E. Molinari, Phys. Rev. B **41**, 9935 (1990).
[20] D. Lim, M. C. Downer, J. G. Ekerdt, N. Arzate, B. S. Mendoza, V. I. Gavrilenko, and R. Q. Wu, Phys. Rev. Lett. **84**, 3406 (2000).
[21] J. L. P. Hughes and J. E. Sipe, Phys. Rev. B **53**, 10751 (1996).
[22] J. E. Sipe and Ed. Ghahramani, Phys. Rev. B **48**, 11705 (1993).
[23] B. S. Mendoza, A. Gaggiotti, and R. Del Sole, Phys. Rev. Lett. **81**, 3781 (1998).
[24] V. I. Gavrilenko, Phys. Status Solidi A **188**, 1267 (2001).
[25] W. G. Schmidt, F. Bechstedt, and J. Bernholc, Phys. Rev. B **63**, 045322 (2001).
[26] T. Uchiyama and M. Tsukada, Phys. Rev. B **53**, 7917 (1996).
[27] A. Pasquarello, M. S. Hybertsen, and R. Car, Phys. Rev. Lett. **74**, 1024 (1995).
[28] G. Erley and W. Daum, Phys. Rev. B **58**, R1734 (1998).
[29] V. I. Gavrilenko, R. Q. Wu, M. C. Downer, J. G. Ekerdt, D. Lim, and P. Parkinson, Thin Solid Films **364**, 1 (2000).
[30] B. S. Mendoza, M. Palummo, G. Onida, and R. Del Sole, Phys. Rev. B **63**, 205406 (2001).